Pseudophyllomitus vesiculosus (Larsen and Patterson 1990) Lee, 2002, a poorly studied phagotrophic biflagellate is the first characterized member of stramenopile environmental clade MAST-6

Takashi Shiratori[a,1], Rabindra Thakur[b], and Ken-ichiro Ishida[a]

[a]Faculty of Life and Environmental Sciences, University of Tsukuba, Tsukuba, Ibaraki 305-8572, Japan

[b] Graduate School of Life and Environmental Sciences, University of Tsukuba, Tsukuba, Ibaraki 305-8572, Japan

Running title: A first characterized member of MAST-6

[1]Corresponding Author: Fax: +81 298 53 4533

E-mail: wb.takashi@gmail.com (T. Shiratori)

Abstract

There are many eukaryotic lineages that exclusively composed of environmental sequences and lack information about which species are included. Regarding stramenopiles, at least 18 environmental lineages, known as marine stramenopiles (MAST), have been recognized. Since each MAST lineage forms deep branches in the stramenopiles, the characterization of MAST members is key to understanding the diversity and evolution of stramenopiles. In this study, we established a culture of *Pseudophyllomitus vesiculosus*, which is a poorly studied phagotrophic flagellate of uncertain taxonomic position. Our molecular phylogenetic analyses based on small subunit ribosomal RNA gene sequences robustly supported the inclusion of *P. vesiculosus* in the MAST-6 clade. Our microscopic observations indicated that *P. vesiculosus* shared characteristics with stramenopiles, including an anterior flagellum that exhibits sinusoidal waves and bears tubular mastigonemes. The flagellar apparatus of *P. vesiculosus* was also similar to other stramenopiles in having a transitional helix and five microtubular roots (R1–R4 and S tubules) including R2 that split into two bands. On the other hand, *P. vesiculosus* was distinguished from other deep-branching stramenopiles by the combination of flagellar apparatus characteristics. Based on the phylogenetic analyses and microscopic observations, we established Pseudophyllomitidae fam. nov in stramenopiles.

Key words: flagellar apparatus; MAST; phylogenetic analysis; stramenopiles; ultrastructure

Introduction

Environmental DNA surveys focusing on small subunit ribosomal RNA (SSU rRNA) gene sequences have uncovered the great diversity of protists (Bass and Cavalier-Smith 2004; Lara et al. 2009; Lopez-Garcia et al. 2001). These environmental DNA surveys have revealed not only the cryptic diversity of previously described taxa (Cavalier-Smith and Von der Heyden, 2007; Holzmann et al. 2003; Lara et al. 2009), but also novel environmental lineages that could not be assigned to any described groups (Choi et al. 2017; Kim et al. 2016). Culture-independent studies, such as fluorescence in situ hybridization (FISH) and single cell based genome sequencing are effective approaches to characterize these environmental lineages, and the methods have provided important information, including cell shape and size, presence or absence of plastids, and mode of nutrition (Jones et al. 2011; Yoon et al. 2011). However, traditional culture-based taxonomic studies are also important for improved characterization of these environmental lineages (del Campo et al. 2016; Moreira and López-García 2014). This approach provides detailed morphological and ultrastructural information that complements culture-independent studies and aids our understanding of the ecological role and evolutionary history of targeted organisms.

Stramenopiles are a large eukaryotic assemblage characterized by the presence of tripartite or bipartite tubular hairs (mastigonemes) on the anterior flagellum, and the group includes various organisms ranging from multicellular seaweeds (Phaeophyceae) and parasitic or saprotrophic fungus-like organisms (e.g., Hyphochytrea and Oomycetes) to diverse photosynthetic and heterotrophic protists (e.g., Bikosea, Chrysophyceae, and

Bacillariophyceae). The stramenopiles also include several environmental lineages that are not classified in any described groups, which have been described as MArine STramenopiles (MAST) or Mystery Heterokont (MH) (Massana et al. 2004; Orsi et al. 2011; Richards and Bass 2005). Massana et al. (2014) rearranged newly and previously described environmental lineages into 18 MAST groups (MAST-1, -2, -3, -4, -6, -7, -8, -9, -10, -11, -12, -16, -20, -21, -22, -23, -24, and -25) by excluding synonyms and lineages that are represented by chimeric sequences.

Molecular phylogenetic analyses using SSU rRNA gene sequences indicated that most MAST lineages formed deep branches within the stramenopiles (Cavalier-Smith and Scoble 2013; Massana et al. 2014). Therefore, the characterization of MAST species is key to understanding the diversity and evolution of stramenopiles. Investigations of MAST species to date have been mainly performed using culture independent approaches. Environmental DNA surveys showed that the abundance of MAST sequences reached around 20% of total picoeukaryotes in the surface water of open oceans (Massana et al. 2004), while some MAST lineages were specific to anaerobic water column or sediment (Massana et al. 2014). FISH experiments using lineage-specific oligonucleotide probes and incubation experiments revealed approximate cell size, habitat, and the prey of some MAST members (Kolodziej and Stoeck 2007; Massana et al. 2009; Piwosz and Pernthaler 2010). On the other hand, culture-dependent approaches for the identification of MAST members have not been frequently performed and only a few MAST species have been identified so far (MAST-3: *Incisomonas marina* and *Solenicola setigera*) (Cavalier-smith and Scoble 2013; Gómez et al. 2011).

In this study, we established a culture of *Pseudophyllomitus vesiculosus* (strain SRT537) from marine detritus on the tidal flat sediment of Amami Island, Okinawa, Japan. *Pseudophyllomitus* is a genus of heterotrophic free-living flagellates established by Lee (2002), and it includes four species that were reassigned from *Phyllomitus* based on morphological differences. *Pseudophyllomitus* has a sac-shaped cell body and two heterodynamic flagella that emerge from a subapical gullet or pocket (Lee 2002). Although *Pseudophyllomitus* spp. were reported in field surveys of marine sediment samples (Aydin and Lee 2012; Larsen and Patterson 1990; Lee 2015; Lee and Patterson 2000), molecular and ultrastructural data of this genus are still unavailable, thus the taxonomic position is uncertain. Our molecular phylogenetic analysis using SSU rRNA gene sequences showed that *P. vesiculosus* is a member of the MAST-6. We also performed microscopic observations of *P. vesiculosus*, and compared the morphology and ultrastructure with other deep-branching stramenopiles for MAST-6 characterization.

Results

Light microscopic observation

The cells of *P. vesiculosus* strain SRT537 were flexible, sac-shaped, and slightly dorsoventrally flattened (Fig. 1A, B). Cell length was 9.3–18.3 μm (13.58 ± 1.95 μm, n = 62), and the width was 6.3–12.4 μm (8.89 ± 1.31 μm, n = 62). Two flagella were inserted subapically, and were arranged at a right angle (Fig. 1A–D). The anterior flagellum was 14.4–24.9 μm (19.31 ± 2.10 μm, n = 58), curved over the right side of the cell, and it exhibited sinusoidal waves during swimming. The posterior flagellum was as long as or slightly longer than the cell, and it trailed behind the cell body. Cells had many large vesicles (approximately 1.1–2.4 μm in diameter) in the peripheral region (Fig. 1A–E). Cells occasionally included lipid globules that were probably derived from prey diatoms (Fig. 1A, B, D). A nucleus with a nucleolus was positioned at the center or slightly anterior region of the cell (Fig. 1A, B). A rod or bar laid against anterior side of the nucleus (Fig. 1A). Cells swam immediately above the substrate with attaching the tip of the posterior flagellum to the substrate or in the water column with rotating movements.

Transmission electron microscopic observation

Whole-mount observation using a transmission electron microscope showed that *P. vesiculosus* strain SRT537 had bipartite tubular mastigonemes on the anterior flagellum (Fig. 1F). The tubular mastigoneme consisted of a shaft and a terminal filament (Fig. 1G, H). The posterior flagellum was acronematic (Fig. 1F).

In ultrathin section observation, thin extensions were observed on the cell surface (Fig, 2A). The extensions considered to be fixation artifacts because they were not observed in light microscopy (Fig. 1A-E) and whole-mount observation (Fig. 1F) as well as

ultrathin section observation using chemical fixation specimen (not shown). Except for the extensions, no appendages (e.g., cell wall, cell coat, and scales) were observed on cell surface (Fig. 2A). A large nucleus with a conspicuous nucleolus was observed at the middle to anterior region of the cell (Fig. 2A). A Golgi apparatus was located at the anterior region of the cell, along the anterior side of the nucleus (Fig. 2A). Large vesicles that occasionally contained amorphous inclusions were arranged along the peripheral region of the cell (Fig. 2A). Several round or oval mitochondrial profiles with tubular cristae were scattered throughout the cell (Fig. 2A, B). Amorphous microbodies, including dense dots were closely associated with the nucleus (Fig. 2C). The endoplasmic reticulum (ER) around the nucleus included bunches of mastigonemes (Fig. 2D). Small vesicles containing electron dense inclusions were observed just beneath the plasma membrane (Fig. 2E).

The flagellar transitional region had a dense transitional plate and a single transitional helix with 10–12 gyros that were positioned at the distal side of the plate (Fig. 3A, B). Two basal bodies were arranged at approximately 70–90° (Fig. 3C, D). The basal bodies were not in the same plane, and the right side of the posterior basal body was closely associated with the left side of the anterior basal body (Fig. 3D). Basal bodies were connected by a fibrous bridge (Fig. 3C, D). Another fibrous structure was associated with the posterior side of the posterior basal body (Fig. 3C, E). This fibrous structure was separated into several bands, and was directed towards the nucleus (Fig. 3E). Since the microtubular roots of *P. vesiculosus* appear to be homologous with those of other stramenopiles, we applied the label for microtubular roots used by Moestrup (2000). The posterior basal body had three microtubular roots (R1, R2, and S tubule). The R2 consisted

of 13 microtubules that were arranged in an L-shape, and the short side was associated with the right side of the posterior basal body (Fig. 3E, F). We numbered each R2 microtubule as described by Moestrup and Thomsen (1976) (1–10 and a–c from the long side to the short side of the L-shape). The R2 was directed towards the posterior side, and it then split into two bands (Fig. 3G–J). The large band that consisted of microtubules 1–10 directed to the right side, whereas the small band that consisted of microtubules a–c directed to the left side of the cell (Fig. 3G–J). The R1 consisted of a single microtubule (Fig. 4A–C). It originated from the anterior side of the posterior basal body and directed to the left side of the cell (Fig. 4A–C). The S tubule consisted of a single microtubule, and it originated from the posterior side of the basal body (Fig. 4A–D). It directed to the left side of the cell, along with the R1 (Fig. 4A–D). The anterior basal body had two microtubular roots (R3 and R4). The R3 consisted of two microtubules (Fig. 4G, H). It originated from the right side of the anterior basal body, and directed to the dorsal right side of the cell (Fig. 4G, H). The R4 consisted of a single microtubule. It originated from the left side of the anterior basal body and directed to the dorsal side of the cell (Fig. 4G, H). The flagellar apparatus of *P. vesiculosus* is illustrated in Fig. 5A.

Molecular phylogenetic analysis

The maximum likelihood (ML) tree based on 113 SSU rRNA gene sequences, including all major groups of stramenopiles and MAST lineages, is shown in Fig. 6. In the ML tree, *P. vesiculosus* formed a clade with seven environmental sequences that were labeled as MAST-6 in Massana et al. (2014) with robust statistical supports. No environmental sequences were identical to *P. vesiculosus*, and nucleotide differences between *P. vesiculosus* and the seven MAST-6 environmental sequences were 5–7%. The MAST-6 clade including *P. vesiculosus* branched as sister group to MAST-20, but the position was not statistically supported.

Discussion

Pseudophyllomitus vesiculosus is a member of MAST-6

Lee (2002) established the genus *Pseudophyllomitus*, and moved four *Phyllomitus* species (*P. apiculatus* Skuja 1948, *P. granulatus* Larsen and Patterson 1990, *P. salinus* Lackey 1940, and *P. vesiculosus*) to the new genus, because they lacked the two adhering flagella that were observed in the type species (*P. undulans* Stein 1878). *Pseudophyllomitus* is characterized by a flexible, sac-shaped cell, and two flagella that do not adhere to each other and inserted sub-apically into a gullet or pocket (Lee 2002). Although *Pseudophyllomitus* spp. have been reported by field surveys (Aydin and Lee 2012; Larsen and Patterson 1990; Lee 2015; Lee and Patterson 2000), no ultrastructural and molecular investigations had been performed on these species. Therefore, their taxonomic position remained uncertain. Our light microscopic observations indicated that the strain SRT537 exhibited characteristics of *Pseudophyllomitus*. The cytoplasm of the strain SRT537 was highly vesiculated, which is a unique characteristic of *P. vesiculosus*. Cell size and swimming behavior of this strain also corresponded with the original description of *P. vesiculosus*. Therefore, we concluded that the strain SRT537 is *P. vesiculosus*.

Our molecular phylogenetic analyses clearly showed that *P. vesiculosus* is a member of the stramenopiles, and this phylogenetic position was also supported by both morphological and ultrastructural characters shared among stramenopiles such as the presence of an anterior flagellum with tubular mastigonemes and a sinusoidal beating pattern as well as a transitional helix in the flagellar transitional region. In the SSU rRNA gene tree, *P. vesiculosus* was included in the MAST-6 clade with robust supports, which indicated that this species is the first recognized member of MAST-6. Although it was

suggested that *Pseudophyllomitus* might not be a coherent genus (Cavalier-Smith 2016; Lee 2002) and it includes a potential kinetoplastid species (*P. apiculatus*), the type species of *Pseudophyllomitus* (*P. granulatus*) has similar morphological characteristics and flagellar orientation to those of *P. vesiculosus*. Moreover, the anterior flagellum of *P. granulatus* also shows sinusoidal waves, which is a characteristic of stramenopiles including *P. vesiculosus* (Lee and Patterson 2000). Therefore, we concluded that *Pseudophyllomitus* should be treated as a member of the stramenopiles, and that it should be placed in the MAST-6. *Pseudophyllomitus apiculatus* probably should be transferred to Kinetoplastida and *P. salinus* needs to be re-examined in detail by molecularly and ultrastructurally in the future. Previous culture-independent studies also supported the placement of *Pseudophyllomitus* in MAST-6. Environmental DNA surveys indicated that MAST-6 sequences were mainly obtained from sediment samples (Logares et al. 2012; Massana et al. 2014), and FISH observations using a specific probe showed that MAST-6 includes at least small (6.4 ± 0.8 μm in length) and large (14.1 ± 2.4 μm in length) morphotypes that fed on algae (Piwosz and Pernthaler 2010). *P. vesiculosus* and *P. granulatus* were detected in sediment samples, and both feed on algae (Aydin and Lee 2012; Larsen and Patterson 1990; Lee and Patterson 2000). Moreover, the cell sizes of *P. vesiculosus* and other *Pseudophyllomitus* spp. corresponded with the large morphotype of MAST-6 that was detected by Piwosz and Pernthaler (2010). On the other hand, the cell size of the small morphotype of MAST-6 detected by Piwosz and Pernthaler (2010) did not overlap with that of *Pseudophyllomitus* spp., and MAST-6 environmental sequences were also obtained from picoplanktonic size fractions and anaerobic environments (Behnke et al. 2006; Logares et al.

2012). We confirmed that the probe used in Piwosz and Pernthaler (2010) has three mismatches to *P. vesiculosus* sequence, suggesting that it detected MAST-6 organisms other than *P. vesiculosus*. These information suggests the possibility that there are still some undescribed genera or species in MAST-6.

Comparison of flagellar apparatus with other basal stramenopiles

Our molecular phylogenetic analyses using SSU rRNA gene sequences failed to resolve the relationship between the MAST-6 clade and other deep-branching stramenopiles. The deep branching stramenopiles comprise six described lineages (Bikosea, Labyrinthulea, Nanomonadea, Opalinata, Placididea, and *Platysulcus*), and three of the six (Bikosea, Placididea, and *Platysulcus*) are groups of free-living biflagellates. These three deep-branching groups are generally small (<10 μm) and feed on bacteria, and this is in contrast with large-celled *P. vesiculosus* that feeds on eukaryotic algae. Since other MAST organisms are also suggested as small and bacterivorous (Massana et al. 2002, 2006), the large cell size and the eukaryovorous behavior are possibly specific features of *Pseudophyllomitus* to distinguish it from other deep-branching stramenopile flagellates. Flagellar apparatus is one of main taxonomic traits for higher classification and these deep-branching stramenopile flagellates also can be clearly distinguished by specific features in their flagellar apparatuses (Fig. 5). Placididea, and *Platysulcus* share microtubular roots R1–R4, including R2 that splits into two rows (Fig. 5B, D). Placididea includes three genera, and two of these genera (*Wobblia* and *Placidia*) have almost identical flagellar apparatuses in that R2 consists of ten (7+3) microtubules that are arranged in a U-shape. Furthermore, the flagellar transitional regions of these two genera exhibit double

transitional helices, and the basal bodies contain intrakinetosomal shelves (Moriya et al. 2000, 2002). The third genus, *Suigetsumonas*, was recently described, and it differed from the other two placididean genera in that it exhibited an R2 with 5+3 microtubules and a single transitional helix, and it lacked intrakinetosomal shelves (Okamura and Kondo 2015). *Platysulcus* includes a single species, *P. tardus*. This species has an R2 with 7+3 microtubules and another singlet microtubule (S tubule) that originates from posterior basal body, and lacks any helical structures in the transitional region and the basal body (Shiratori et al. 2015). Flagellar apparatuses of bikosean flagellates had been considered to have similar microtubular root system with Placididea and *Platysulcus*. However, Harder et al. (2014) argued that the split R2 has different origins and they should be treated as separate roots, R2 and R3 respectively (Fig. 5C). The R3+R2 (former split R2) consists of 8 (R3)+3 (R2) microtubules. However, the number of microtubules in R2+R3 varies among species (e.g., 6+3 in *Symbiomonas scintillans*, 3+1 in *Siluania monomastiga*, and 10+1 in *Otto terricolus*) (Guillou et al. 1999; Harder et al. 2014; Karpov et al. 1998; 2001). Bikosean flagellates are mostly characterized by the presence of an additional singlet microtubule (x-fiber) that is associated with R2. Furthermore, another singlet microtubule (S tubule) that originates from posterior basal body was reported in *Bicosoeca maris* (Moestrup and Thomsen 1976). S tubule is also reported in *Rictus lutensis*, an anaerobic flagellate that might be a member of Bikosea. (Yubuki et al. 2010) In some bikoseans species, concentric rings or spiral fibers were reported in their flagellar transitional region (Karpov 2000; Karpov et al. 1998). Our ultrathin section observations of *P. vesiculosus* indicated that it has microtubular roots R1–R4, including a split R2 that is similar to other

deep-branching stramenopile flagellates. On the other hand, the R2 of *P. vesiculosus* has 13 microtubules (10+3); this has not been reported in other deep-branching stramenopiles. *P. vesiculosus* also differs from bikoseans in that it lacks an x-fiber. Similarly, *P. vesiculosus* possesses an S tubule that is not found in placidideans, and it has only been reported in a few bikosean species and *Platysulcus*. *P. vesiculosus* also has a single transitional helix that is absent in *Platysulcus*. Additionally, *P. vesiculosus* lacks some ultrastructural characteristics that are observed in Labyrinthulea and Opalinata, including a bell-shaped structure in the flagellar transitional region and intrakinetosomal shelves in the basal bodies (Barr and Allan 1985; Patterson and Delvinquier 1990). The combination of ultrastructural characteristics in the flagellar apparatus can separate *P. vesiculosus* from other deep-branching stramenopiles. Our molecular phylogenetic analyses suggested that *P. vesiculosus* is an independent lineage of deep-branching stramenopiles, and this is congruent with its unique ultrastructure. Based on the phylogenetic position and ultrastructure, we propose a new family Pseudophyllomitidae fam. nov. in stramenopiles.

Taxonomic Summary

Pseudophyllomitidae fam. nov. (ICZN)

Pseudophyllomitaceae fam. nov. (ICN)

Diagnosis: Free-living phagotrophic biflagellates. Anterior flagellum bears tubular mastigonemes. Mitochondria with tubular cristae. Flagellar transitional region with transitional helix. S tubule and split R2 present.

Type species: *Pseudophyllomitus granulatus*.

Materials and methods

Culture establishment: Marine detritus was collected from the tidal flat of Amami Island, Kagoshima, Japan (28.441809 °N, 129.671856 °E). The detritus was incubated for six days in mIMR medium (Kasai 2009) at 20 °C under a 14 h light and 10 h dark cycle. A cell of *P. vesiculosus* in the incubated sample was isolated by micropipetting and was placed into a 96-well plate containing a pennate diatom culture in mIMR medium. A established culture of *P. vesiculosus* (strain SRT537) was maintained in ESM medium (Kasai 2009) by adding *Chaetoceros* sp. or *Phaeodactylum tricornutum* as prey at 18 °C under a 14 h light and 10 h dark cycle. The strain SRT537 was deposited at the National Institute for the Environmental Sciences (NIES), Tsukuba, Japan as NIES-4114.

Light and electron microscopic observations: The cells of the strain SRT537 were observed using an Olympus IX71 inverted microscope (Olympus, Tokyo, Japan) that was equipped with an Olympus DP71 CCD camera (Olympus).

For the observations of whole-mount cells using transmission electron microscopy (TEM), cell suspensions were mounted on formvar-coated copper grids, and were fixed using OsO_4 vapor. The copper grids were washed with distilled water and stained with 2% (w/v) uranyl acetate. The grids were then observed using a Hitachi H-7650 electron microscope (Hitachi High-Technologies Corp., Tokyo, Japan) that was equipped with a Veleta TEM CCD camera (Olympus).

Specimens for ultrathin section observation using TEM were prepared as follow; pellets of centrifuged cells were placed on a formvar-coated copper loop and plunged rapidly into liquid propane. The frozen pellets were then plunged into liquid nitrogen for

several seconds and were then placed in acetone with 2% osmium tetroxide at -85 °C for 48 h. The fixing solution was kept at -20 °C for 2 h and at -4 °C for 2 h. The pellets were rinsed with acetone three times, and were then replaced by agar low viscosity resin R1078 (Agar Scientific Ltd, Stansted, England). The resin was polymerized by heating at 60°C for 12 h. Ultrathin sections were prepared on a Reichert Ultracut S ultramicrotome (Leica, Vienna, Austria), and were double stained with 2% (w/v) uranyl acetate and lead citrate (Hanaichi et al. 1986; Sato 1968). Ultrathin sections were then observed using a Hitachi H-7650 electron microscope (Hitachi High-Technologies Corp.) that was equipped with a Veleta TEM CCD camera (Olympus).

DNA extraction and polymerase chain reaction (PCR): Cells of the strain SRT537 were centrifuged, and total DNA was extracted from the pellet using a DNeasy Plant Mini Kit (Qiagen Science, Valencia, CA), according to the manufacturer's instructions. The SSU rRNA gene sequence of the strain SRT537 was amplified via polymerase chain reaction (PCR) with 18F-18R primers (Yabuki et al. 2010). Amplification consisted of 30 cycles of denaturation at 94°C for 30 s, annealing at 55°C for 30 min, and extension at 72°C for 2 min. An additional extension at 72°C for 4 min was performed at the end of the reaction. Amplified DNA fragments were subjected to gel electrophoresis, and were then purified using a QIAquick Gel Extraction Kit (Qiagen Science). Purified products were then cloned into the p-GEM® T-easy vector (Promega, Tokyo, Japan), and the inserted DNA fragments were completely sequenced using a 3130 Genetic Analyzer (Applied Biosystems, Monza, Italy). The SSU rDNA sequence of the strain SRT537 was deposited as LC257669 in GenBank.

Sequence alignments and phylogenetic analyses: we newly created a dataset of SSU rRNA gene sequences that includes 104 stramenopiles that represent all major lineages and MAST clades, and nine alveolates and rhizarians as outgroups. Our newly obtained SSU rRNA gene sequence of the strain SRT537 was added to this dataset. All sequences were automatically aligned using MAFFT (Katoh and Standley 2013), and the resulting alignment was manually edited using SeaView (Gouy et al. 2010). For phylogenetic analyses, ambiguously aligned regions were manually deleted from the alignment, resulting in an SSU rDNA alignment with 1,570 nucleotide positions. The alignment file used in this analysis is available upon request. ML analyses were performed with IQ-TREE v. 1.3.0 (Nguyen et al. 2015), and the model that best fit the data was determined based on the Bayesian information criterion (BIC). The best-fit model for our dataset was TIM2+I+G4. To assess branch support, 100 replicates of non-parametric bootstrap analysis was performed using IQ-TREE. A Bayesian analysis was also conducted using MrBayes v. 3.2.2 (Ronquist et al 2012) with the GTR+I+G4 model. One cold and three heated Markov chains with default temperature parameters were run for 6.1×10^7 generations, and trees were sampled at 100 generation intervals. Convergence was assessed based on the average standard deviation of split frequencies, and the first 25% of each generation was discarded as "burn-in." Bayesian posterior probabilities and branch lengths were calculated from the remaining trees.

Acknowledgments

This work was supported by JSPS KAKENHI Grant Number 13J00587.

References

Aydin EE, Lee WJ (2012) Free-living heterotrophic flagellates from intertidal sediments of Saros Bay, Aegean Sea (Turkey). Acta Protozool **51**:119–137

Barr DJS, Allan PME (1985) A comparison of the flagellar apparatus in *Phytophthora*, *Saprolegnia*, *Thraustochytrium*, and *Rhizidiomyces*. Can J Bot **63**:138–154

Bass D, Cavalier-Smith T (2004) Phylum-specific environmental DNA analysis reveals remarkably high global biodiversity of Cercozoa (Protozoa). Int J Syst Evol Microbiol **54**:2393–2404

Behnke A, Bunge J, Barger K, Breiner HW, Alla V, Stoeck T (2006) Microeukaryote community patterns along an O_2/H_2S gradient in a supersulfidic anoxic fjord (Framvaren, Norway). Appl Environ Microbiol **72**:3626–3636

Cavalier-Smith T (2016) Higher classification and phylogeny of Euglenozoa. Eur J Protistol **56**:250–276

Cavalier-Smith T., von der Heyden S (2007) Molecular phylogeny, scale evolution and taxonomy of centrohelid heliozoa. Mol Phylogenet Evol **44**:1186–1203

Cavalier-Smith T, Scoble JM (2013) Phylogeny of Heterokonta: *Incisomonas marina*, a uniciliate gliding opalozoan related to *Solenicola* (Nanomonadea), and evidence that Actinophryida evolved from raphidophytes. Eur J Protistol **49**:328–353

Choi CJ, Bachy C, Jaeger GS, Poirier C, Sudek L, Sarma VVSS, Mahadevan A, Giovannoni SJ, Worden AZ (2017) Newly discovered deep-branching marine plastid lineages are numerically rare but globally distributed. Curr Biol **27**: R15–R16

del Campo J, Guillou L, Hehenberger E, Logares R, López-García P, Massana R (2016) Ecological and evolutionary significance of novel protist lineages. Eur J Protistol **55**:4–11

Gómez F, Moreira D, Benzerara K, López-García P (2011) *Solenicola setigera* is the first characterized member of the abundant and cosmopolitan uncultured marine stramenopile group MAST-3. Environ Microbiol **13**:193–202

Gouy M, Guindon S, Gascuel O (2010) SeaView version 4: a multiplatform graphical user interface for sequence alignment and phylogenetic tree building. Mol Biol Evol **27:**221–224

Guillou L, Chretiennot-Dinet MJ, Boulben S, Moon-van der Staay SY, Vaulot D (1999) *Symbiomonas scintillans* gen. et sp. nov. and *Picophagus flagellatus* gen. et sp. nov. (Heterokonta): two new heterotrophic flagellates of picoplanktonic size. Protist **150**:383–398

Hanaichi T, Sato T, Hoshino M, Mizuno N (1986) A stable lead stain by modification of Sato's method. Proceedings of the XIth International Congress on Electron Microscopy, Japanese Society for Electron Microscopy, Kyoto, Japan, pp 2181–2182

Harder CB, Ekelund F, Karpov SA (2014) Ultrastructure and phylogenetic position of *Regin rotiferus* and *Otto terricolus* genera et species novae (Bicosoecida. Heterokonta/Stramenopiles). Protist **165**:144–160

Holzmann M, Habura A, Giles H, Bowser SS, Pawlowski J (2003) Freshwater foraminiferans revealed by analysis of environmental DNA samples. J Eukaryot Microbiol **50**:135–139

Jones MDM, Forn I, Gadelha C, Egan MJ, Bass D, Massana R, Richards TA (2011) Discovery of novel intermediate forms redefines the fungal tree of life. Nature **474**:200–203

Karpov SA (2000) Ultrastructure of the aloricate bicosoecid *Pseudobodo tremulans*, with revision of the order Bicosoecida. Protistology **1**:101–109

Karpov SA, Kersanach R, Williams DM (1998) Ultrastructure and 18S rRNA gene sequence of a small heterotrophic flagellate *Siluania monomastiga* gen. et sp. nov. (Bicosoecida). Eur J Protistol **34**:415–425

Karpov SA, Sogin ML, Silberman JD (2001) Rootlet homology, taxonomy, and phylogeny of bicosoecids based on 18S rRNA gene sequences. Protistology **2**:34–47

Kasai F, Kawachi M, Erata M, Mori F, Yumoto K, Sato M, Ishimoto M (2009) NIES-Collection. List of strains. (8th ed.). Jpn J Phycol (Sôrui) **57**:1–350

Katoh K, Standley DM (2013) MAFFT multiple sequence alignment software version 7: improvements in performance and usability. Mol Biol Evol **30**:772–780

Kim E, Sprung B, Duhamel S, Filardi C, Kyoon Shin M (2016) Oligotrophic lagoons of the South Pacific Ocean are home to a surprising number of novel eukaryotic microorganisms. Environ Microbiol **18**:4549–4563

Kolodziej K, Stoeck T (2007) Cellular identification of a novel uncultured marine stramenopile (MAST-12 clade) small-subunit rRNA gene sequence from a Norwegian estuary by use of fluorescence in situ hybridization-scanning electron microscopy. Appl Environ Microbiol **73**:2718–2726

Lara E, Moreira D, Vereshchaka A, López-García P (2009) Pan-oceanic distribution of new highly diverse clades of deep- sea diplonemids. Environ Microbiol **11**:47–55

Larsen J, Patterson DJ (1990) Some flagellates (Protista) from tropical marine sediments. J Nat Hist **24**:801–937

Lee WJ (2002) Redescription of the rare heterotrophic flagellate (Protista) - *Phyllomitus undulans* Stein, 1878, and erection of a new genus – *Pseudophyllomitus* gen. n. Acta Protozool **41**:375–381

Lee WJ (2015) Small free-living heterotrophic flagellates from marine sediments of Gippsland Basin, South-Eastern Australia. Acta Protozool **54**:53–76

Lee WJ, Patterson DJ (2000) Heterotrophic flagellates (Protista) from marine sediments of Botany Bay, Australia. J Nat Hist **34**:483–562

Logares R, Audic S, Santini S, Pernice MC, de Vargas C, Massana R (2012) Diversity patterns and activity of uncultured marine heterotrophic flagellates unveiled with pyrosequencing. ISME J **6**:1823–1833

López-García P, Rodíiguez-Valera F, Pedrós-Alió C, Moreira D (2001) Unexpected diversity of small eukaryotes in deep-sea Antarctic plankton. Nature **409**:603–607

Massana R, Castresana J, Balague V, Guillou L, Romani K, Groisillier A, Valentin K, Pedrós-Alió C (2004) Phylogenetic and ecological analysis of novel marine stramenopiles. Appl Environ Microbiol **70**: 3528–3534

Massana R, del Campo J, Sieracki ME, Audic S, Logares R (2014) Exploring the uncultured microeukaryote majority in the oceans: reevaluation of ribogroups within

stramenopiles. ISME J **8**:854–866

Massana R, Guillou L, Díez B, Pedrós-Alió C (2002) Unveiling the organisms behind novel eukaryotic ribosomal DNA sequences from the ocean. Appl Environ Microbiol **68**:4554–4558

Massana R, Guillou L, Terrado R, Forn I, Pedrós-Alió C (2006) Growth of uncultured heterotrophic flagellates in unamended seawater incubations. Aquat Microb Ecol **45**:171–180

Massana R, Unrein F, Rodríguez-Martínez R, Forn I, Lefort T, Pinhassi J, Not F (2009) Grazing rates and functional diversity of uncultured heterotrophic flagellates. ISME J **3**:588–596

Moestrup Ø (2000) The Flagellate Cytoskeleton: Introduction of a General Terminology for Microtubular Roots in Protists. In Leadbeater BS, Green JC (eds) The Flagellates: Unity, Diversity and Evolution. Taylor and Francis, London, pp 69–94

Moestrup Ø, Thomsen HA (1976) Fine structural studies of the flagellate genus *Bicoeca* I. – *Bicoeca maris* with particular emphasis on the flagellar apparatus. Protistologica **12**:101–120

Moreira D, López-García P (2014) The rise and fall of Picobiliphytes: how assumed autotrophs turned out to be heterotrophs. Bioessays **36**:468–474

Moriya M, Nakayama T, Inouye I (2000) Ultrastructure and 18S rDNA sequence analysis of *Wobblia lunata* gen. et sp. nov., a new heterotrophic flagellate (Stramenopiles, Incertae sedis). Protist **151**:41–55

Moriya M, Nakayama T, Inouye I (2002) A new class of the stramenopiles, Placididea classis nova: description of *Placidia cafeteriopsis* gen. et sp. nov. Protist **153**:143–156

Nguyen LT, Schmidt HA, von Haeseler A, Minh BQ (2015) IQ-TREE: a fast and effective stochastic algorithm for estimating maximum-likelihood phylogenies. Mol Biol Evol **32**:268–274

Patterson DJ, Delvinquier BLJ (1990) The fine structure of the cortex of the protist *Protoopalina australis* (Slopalinida, Opalinidae) from *Litoria nasuta* and *Litoria inermis* (Amphibia: Anura: Hylidae) in Queensland, Australia. J Protozool **37**:449–455

Piwosz K, Pernthaler J (2010) Seasonal population dynamics and trophic role of planktonic nanoflagellates in coastal surface waters of the Southern Baltic Sea. Environ Microbiol **12**:364–377

Okamura T, Kondo R (2015). *Suigetsumonas clinomigrationis* gen. et sp. nov., a novel facultative anaerobic nanoflagellate isolated from the Meromictic Lake Suigetsu, Japan. Protist **166**:409–421

Orsi W, Edgcomb V, Jeon S, Leslin C, Bunge J, Taylor GT, Varela R, Epstein S (2011) Protistan microbial observatory in the Cariaco Basin, Caribbean. II. Habitat specialization. ISME J **5**:1357–1373

Richards TA, Bass D (2005) Molecular screening of free-living microbial eukaryotes: Diversity and distribution using a meta-analysis. Curr Opin Microbiol **8**:240–252

Ronquist F, Teslenko M, von der Mark P, Ayres DL, Darlig A, Höhna S, Larget B, Liu L, Suchard MA, Huelsenbeck JP (2012) MrBayes 3.2: efficient Bayesian phylogenetic inference and model choice across a large model space. Syst Biol **61**:539–542

Sato T (1968) A modified method for lead staining of thin sections. J Electron Microsc **17**:158–159

Shiratori T, Nakayama T, Ishida K (2015) A new deep-branching stramenopile, *Platysulcus tardus* gen. nov., sp. nov. Protist **166**:337–348

Yabuki A, Inagaki Y, Ishida K (2010) *Palpitomonas bilix* gen. et sp. nov.: a novel deep-branching heterotroph possibly related to Archaeplastida or Hacrobia. Protist **161**:523–538

Yoon HS, Price DC, Stepanauskas R, Rajah VD, Sieracki ME, Wilson WH, Yang EC, Duffy S, Bhattacharya D (2011) Single-cell genomics reveals organismal interactions in uncultivated marine protists. Science 332:714–717

Yubuki N, Leander BS, Silberman JD (2010) Ultrastructure and molecular phylogenetic position of a novel phagotrophic stramenopile from low oxygen environments: *Rictus lutensis* gen. et sp. nov. (Bicosoecida, incertae sedis). Protist **161**:264–278

Figure 1. Light and transmission electron micrographs of *Pseudophyllomitus vesiculosus* strain SRT537. AF, anterior flagellum; L, lipid globule; PF, posterior flagellum; V, large vacuole. Arrowhead indicates a short rod structure associated with the anterior side of the nucleus. **A–E.** Differential interference contrast (DIC) micrographs. Scale bar = 10 μm. **F.** Whole-mount transmission electron micrograph of whole cell. Scale bar = 5 μm. **H.** Whole-mount transmission electron micrograph of the anterior flagellum and mastigonemes. Scale bar = 1 μm **G.** whole-mount transmission electron micrograph of tip of mastigonemes. Scale bar = 500 nm.

Figure 2. Transmission electron micrographs of *Pseudophyllomitus vesiculosus* strain SRT537. G, Golgi apparatus; L, lipid globule; Mt, mitochondrion; Mb, microbody; N, nucleus; n, nucleolus; V, large vacuole. Asterisks indicate tubular mastigonemes in the endoplasmic reticulum (ER). **A.** General cell image. Scale bar = 1 μm. **B.** Mitochondrion. Scale bar = 500 nm. **C.** High magnification view of the nucleus and the microbody. Scale bar = 500 nm. **D.** Nucleus and tubular mastigonemes in the ER. Scale bar = 500 nm. **E.** Small vesicles containing dense materials. Scale bar = 500 nm.

Figure 3. Transmission electron micrographs of *Pseudophyllomitus vesiculosus* strain SRT537. AB, anterior basal body; FB, fibrous bridge; Mt, mitochondrion; PB, posterior basal body. Double arrowheads indicate fibrous structures. A. Cross-section of the flagellar transitional region. Scale bar = 200 nm. **B.** Longitudinal section of the basal body and the flagellar transitional region. Scale bar = 200 nm. C. Approximate longitudinal section of

anterior and posterior basal body. Scale bar = 500 nm. **D.** Approximate cross-section of anterior basal body and approximate longitudinal section of posterior basal body. Scale bar = 500 nm. **E.** Fibrous structure associated with posterior basal body. Scale bar = 500 nm. F. Cross-section of R2 showing 13 microtubules (1–10 and a–c). Scale bar = 200 nm. **G.** R2 that split into two bands. Scale bar = 1 μm. **H**–**J**. Selected serial sections taken from right to left, showing R2 that split into large (1–10) and small (a–c) bands. Scale bar = 500 nm.

Figure 4. Transmission electron micrographs of *Pseudophyllomitus vesiculosus* strain SRT537. AB, anterior basal body; Mt, mitochondrion; S, S tubule; PB, posterior basal body; Double arrowheads indicate fibrous structures. A–H. Selected serial sections taken from ventral to dorsal. Scale bar = 500 nm. I–K. Selected serial sections taken from anterior to posterior. Scale bar = 500 nm.

Figure 5. Illustration of the microtubular roots of stramenopile flagellates. **A.** *Pseudophyllomitus vesiculosus* strain SRT537. **B.** Wobblia lunata, illustrated based on Moriya et al. (2000). Each microtubular root was numbered according to Moestrup (2000). **C.** *Cafeteria roenbergensis* illustrated based on O'kelly and Patterson (1996). Each microtubular root was numbered according to Harder et al. (2014). **D.** *Platysulcus tardus* illustrated based on Shiratori et al. (2015).AB, anterior basal body; FB, fibrous bridge; FS, fibrous structure; PB, posterior basal body; S, S tubule; X, x-fiber.

Figure 6. Maximum-likelihood tree of 104 stramenopiles, four rhizarians, and five

alveolates using 1,570 positions of the small subunit (SSU) rDNA sequences. Environmental sequences were labeled with accession numbers. Only bootstrap support values ≥50% are shown. Nodes supported by Bayesian posterior probabilities ≥0.98 are highlighted with bold lines.

Fig. 1

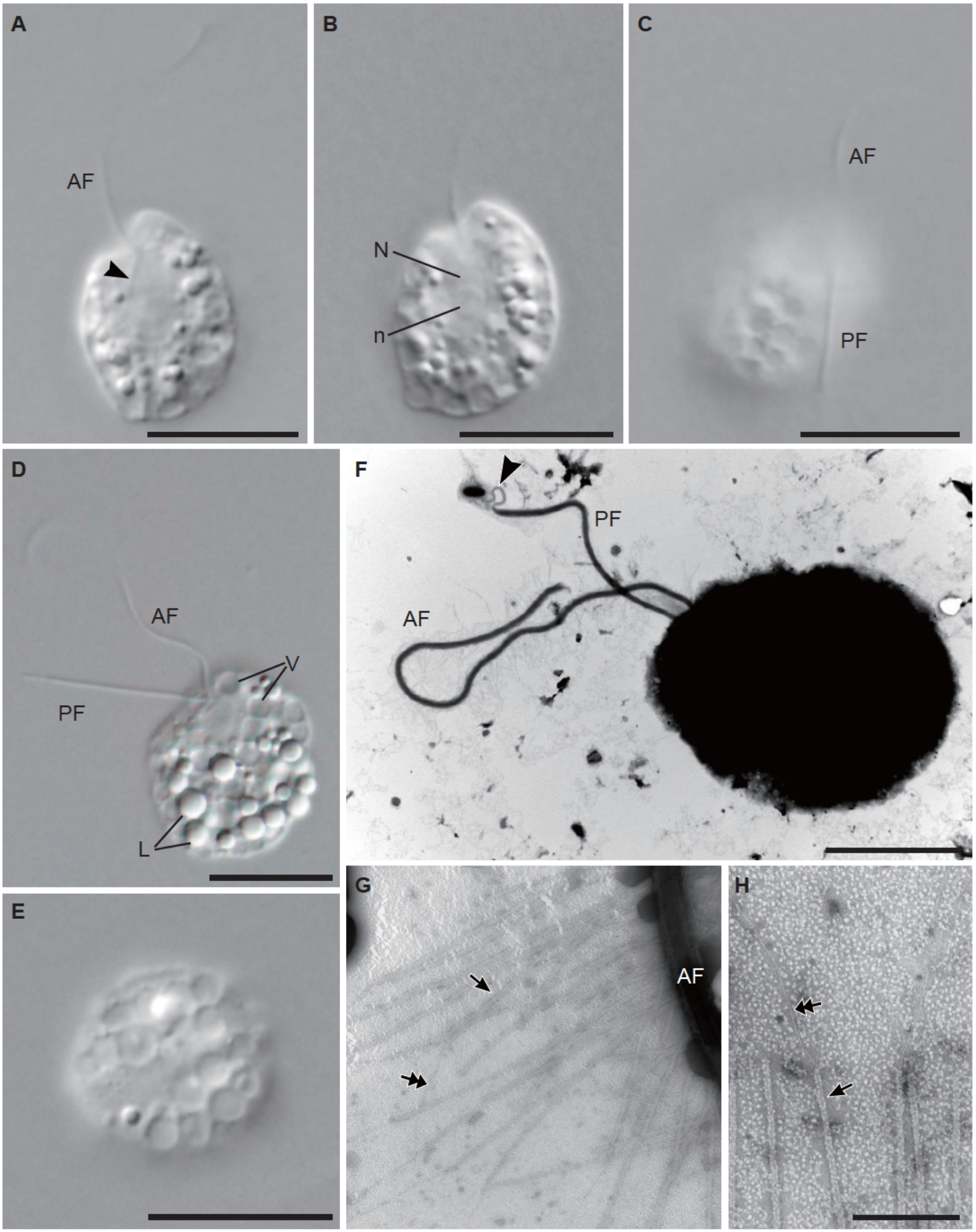

Fig. 2

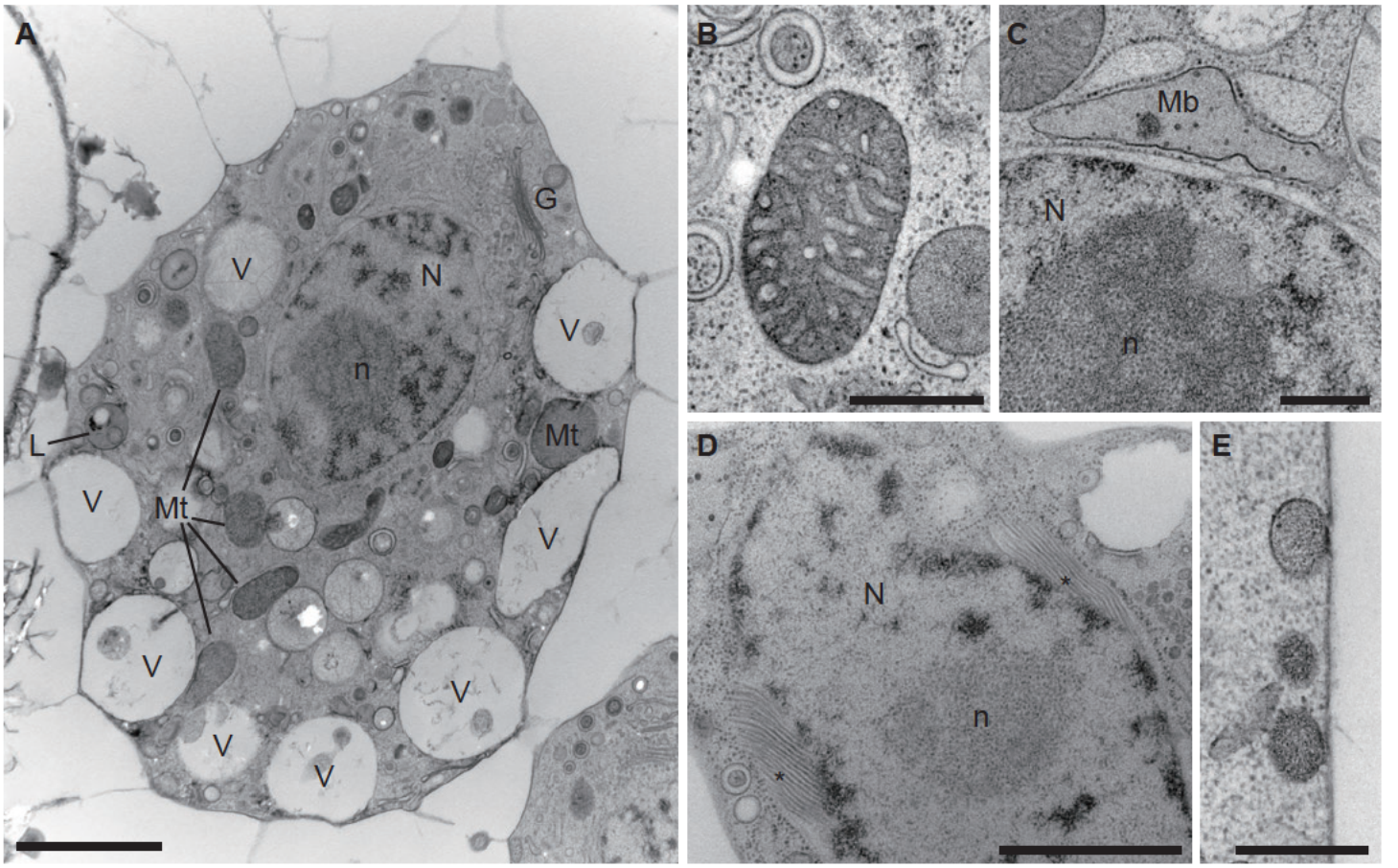

Fig. 3

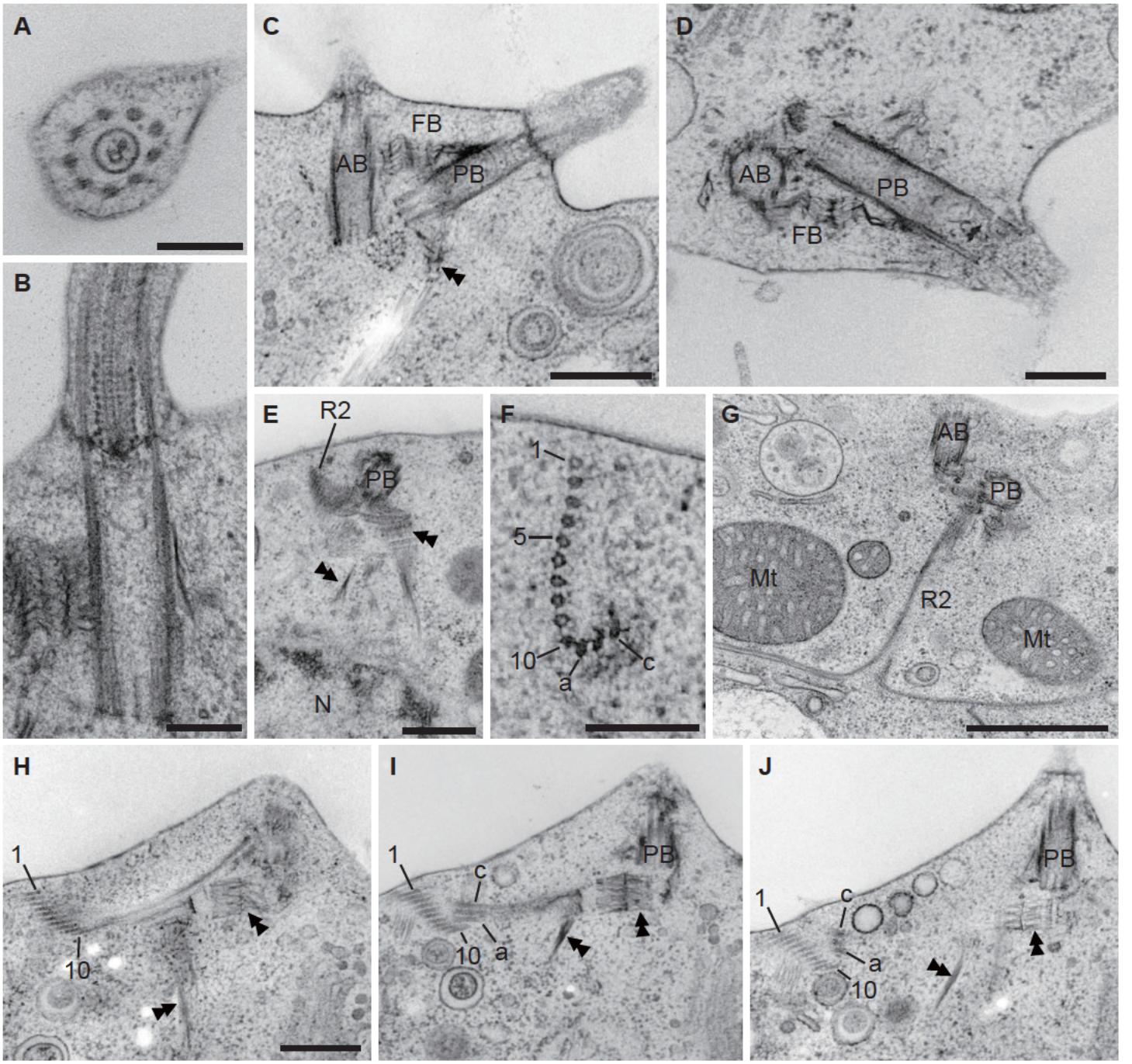
A
B
C
FB
AB
PB
D
AB
PB
FB
E
R2
PB
N
F
1
5
10
a
c
G
AB
PB
Mt
R2
Mt
H
1
10
I
1
c
PB
10
a
J
PB
1
c
a
10

Fig. 4

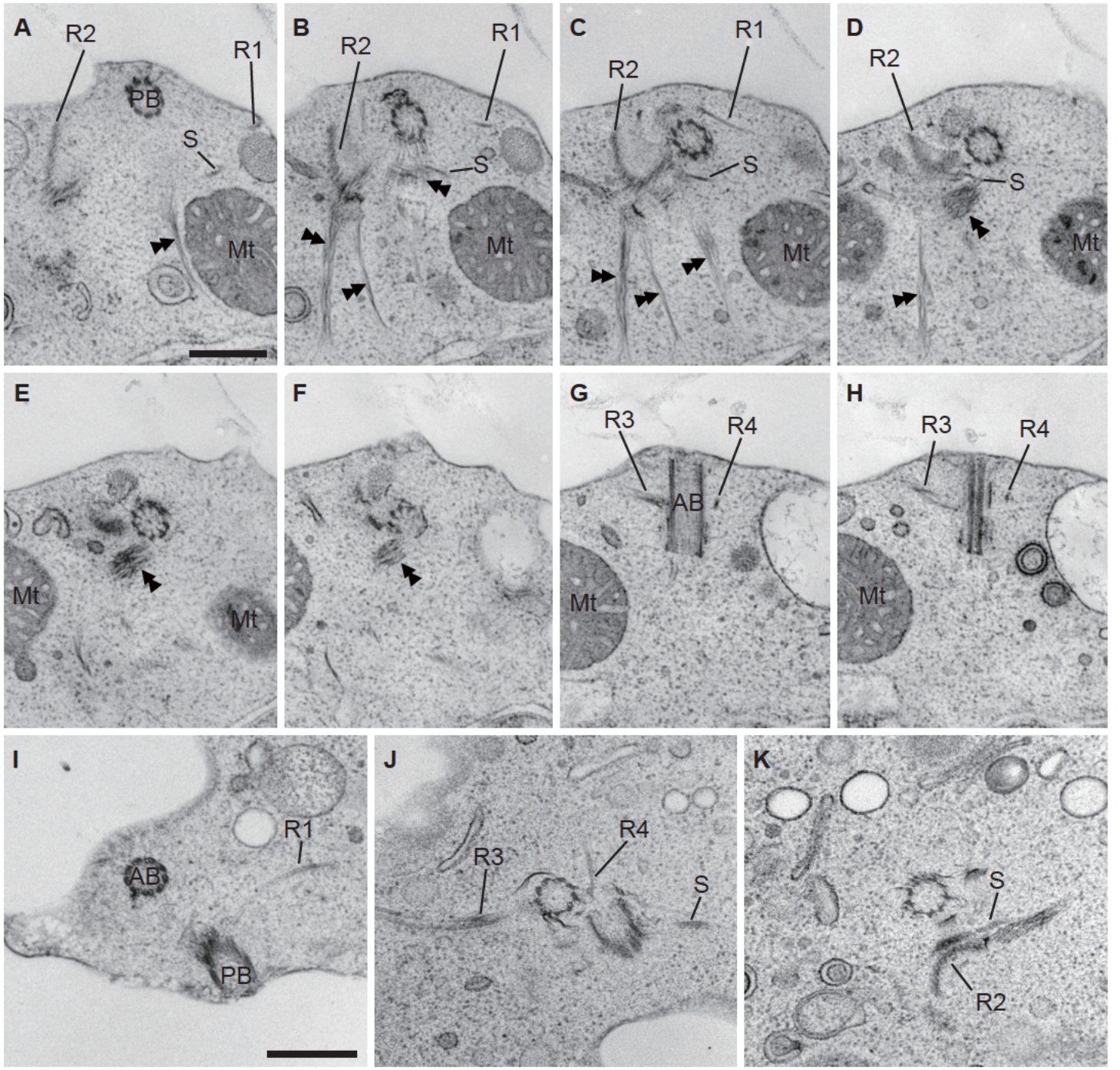
A
R2
R1
PB
S
Mt
B
R2
R1
S
Mt
C
R1
R2
S
Mt
D
R2
S
Mt
E
Mt
Mt
F
G
R3
R4
AB
Mt
H
R3
R4
Mt
I
R1
AB
PB
J
R4
R3
S
K
S
R2

Fig. 5

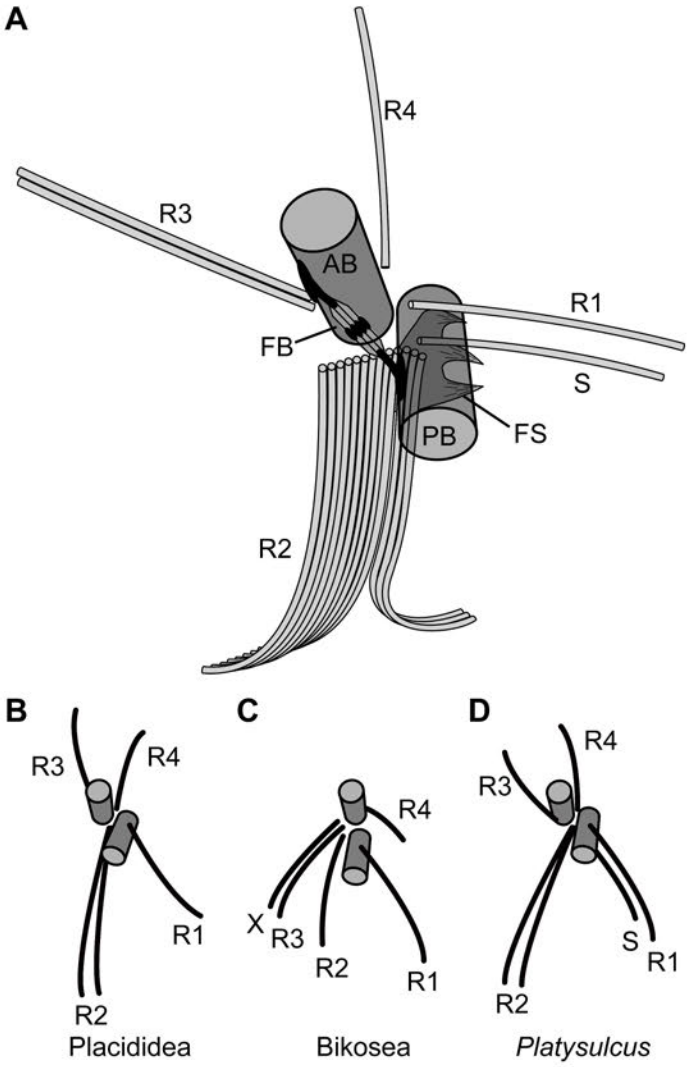
A
R4
R3
AB
R1
FB
S
PB
FS
R2
B
R3
R4
R1
R2
Placididea
C
R4
X
R3
R2
R1
Bikosea
D
R4
R3
S
R1
R2
Platysulcus

Fig. 6

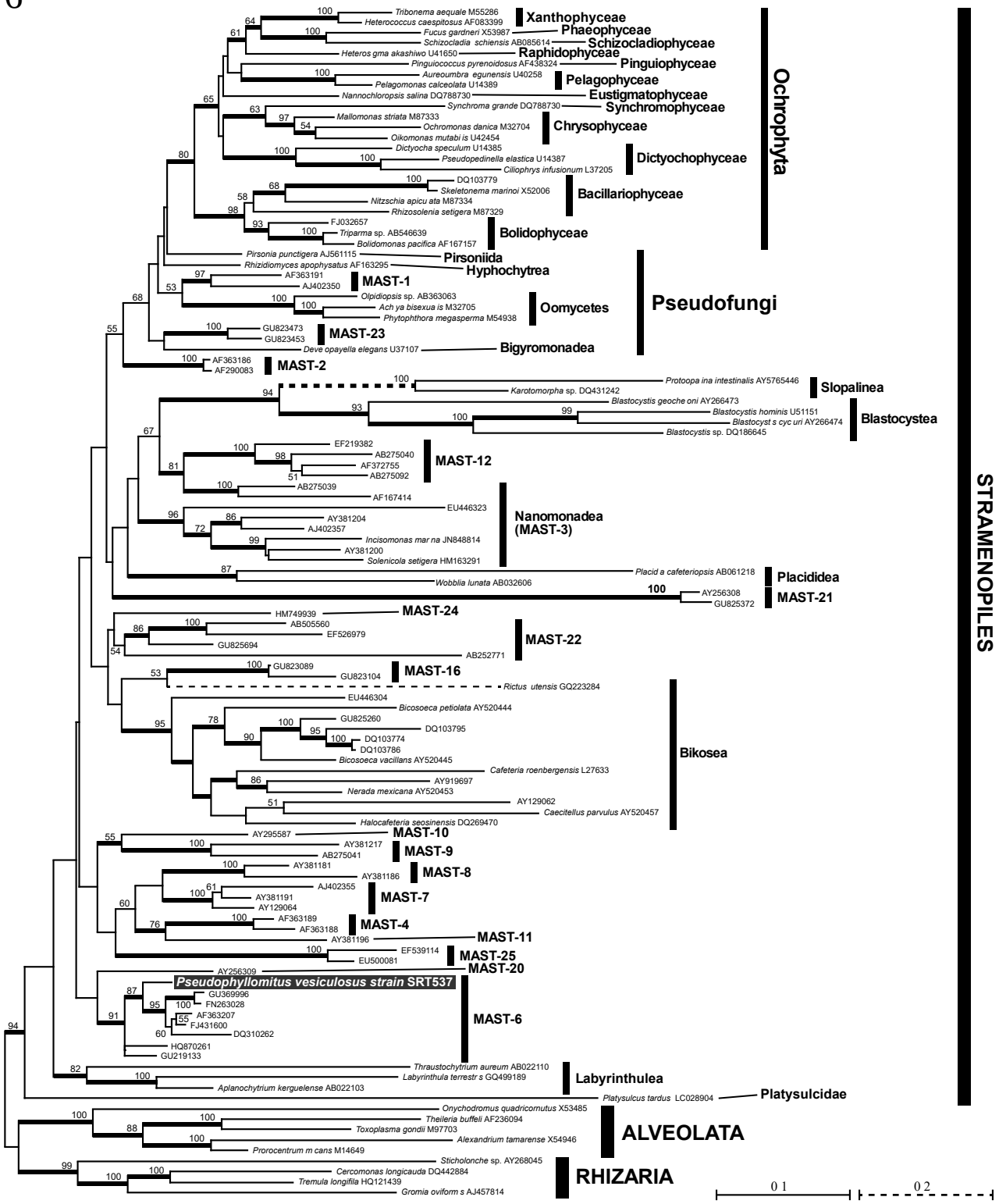
Tribonema aequale M55286
Heterococcus caespitosus AF083399
Xanthophyceae
Fucus gardneri X53987
Phaeophyceae
Schizocladia schiensis AB085614
Schizocladiophyceae
Heteros gma akashiwo U41650
Raphidophyceae
Pinguiococcus pyrenoidosus AF438324
Pinguiophyceae
Aureoumbra egunensis U40258
Pelagomonas calceolata U14389
Pelagophyceae
Nannochloropsis salina DQ788730
Eustigmatophyceae
Synchroma grande DQ788730
Synchromophyceae
Mallomonas striata M87333
Ochromonas danica M32704
Oikomonas mutabi is U42454
Chrysophyceae
Dictyocha speculum U14385
Pseudopedinella elastica U14387
Ciliophrys infusionum L37205
Dictyochophyceae
Ochrophyta
DQ103779
Skeletonema marinoi X52006
Nitzschia apicu ata M87334
Rhizosolenia setigera M87329
Bacillariophyceae
FJ032657
Triparma sp. AB546639
Bolidomonas pacifica AF167157
Bolidophyceae
Pirsonia punctigera AJ561115
Pirsoniida
Rhizidiomyces apophysatus AF163295
Hyphochytrea
AF363191
AJ402350
MAST-1
Olpidiopsis sp. AB363063
Ach ya bisexua is M32705
Phytophthora megasperma M54938
Oomycetes
Pseudofungi
GU823473
GU823453
MAST-23
Deve opayella elegans U37107
Bigyromonadea
AF363186
AF290083
MAST-2
Protoopa ina intestinalis AY5765446
Karotomorpha sp. DQ431242
Slopalinea
Blastocystis geoche oni AY266473
Blastocystis hominis U51151
Blastocyst s cyc uri AY266474
Blastocystis sp. DQ186645
Blastocystea
EF219382
AB275040
AF372755
AB275092
MAST-12
AB275039
AF167414
EU446323
AY381204
AJ402357
Incisomonas mar na JN848814
AY381200
Solenicola setigera HM163291
Nanomonadea
(MAST-3)
Placid a cafeteriopsis AB061218
Wobblia lunata AB032606
Placididea
AY256308
GU825372
MAST-21
STRAMENOPILES
HM749939
MAST-24
AB505560
EF526979
GU825694
AB252771
MAST-22
GU823089
GU823104
MAST-16
Rictus utensis GQ223284
EU446304
Bicosoeca petiolata AY520444
GU825260
DQ103795
DQ103774
DQ103786
Bicosoeca vacillans AY520445
Cafeteria roenbergensis L27633
AY919697
Nerada mexicana AY520453
AY129062
Caecitellus parvulus AY520457
Halocafeteria seosinensis DQ269470
Bikosea
AY295587
MAST-10
AY381217
AB275041
MAST-9
AY381181
AY381186
MAST-8
AJ402355
AY381191
AY129064
MAST-7
AF363189
AF363188
MAST-4
AY381196
MAST-11
EF539114
EU500081
MAST-25
AY256309
MAST-20
Pseudophyllomitus vesiculosus strain SRT537
GU369996
FN263028
AF363207
FJ431600
DQ310262
HQ870261
GU219133
MAST-6
Thraustochytrium aureum AB022110
Labyrinthula terrestr s GQ499189
Aplanochytrium kerguelense AB022103
Labyrinthulea
Platysulcus tardus LC028904
Platysulcidae
Onychodromus quadricornutus X53485
Theileria buffeli AF236094
Toxoplasma gondii M97703
Alexandrium tamarense X54946
Prorocentrum m cans M14649
ALVEOLATA
Sticholonche sp. AY268045
Cercomonas longicauda DQ442884
Tremula longifila HQ121439
Gromia oviform s AJ457814
RHIZARIA
0 1
0 2